Res. Lett. Inf. Math. Sci., 2003, Vol.**5**, pp 129-142
Available online at http://iims.massey.ac.nz/research/letters/

Agglomerate Properties

P. R. Rynhart[1] , J. R. Jones[2] & R. McKibbin[3]

[1] *Institute of Fundamental Sciences*
Massey University, Palmerston North, New Zealand.

[2] *Institute of Technology & Engineering*
Massey University, Palmerston North, New Zealand.

[3] *Institute of Information & Mathematical Sciences*
Massey University at Albany, Auckland, New Zealand.

Modelling of wet granulation requires the rate of agglomerate coalescence to be estimated. Coalescence is dependent on the frequency of collisions that occur, and the fraction of collisions which result in coalescence. The collision rate is a function of granulator kinetics and powder properties, while the coalescence success rate is dependent on factors including the Stokes number and particle geometry. This work investigates an aspect of the geometry by examining the distribution of liquid on the surface of agglomerates in the capillary state. Agglomerates are created by adding particles, one at a time, about a central tetrahedral arrangement of four primary particles. For a given agglomerate, the wetted fraction of surface area, defined as the wetness, is evaluated using an approximate fluid surface. Packing density and binder saturation parameters are incorporated into the model. Given a number of primary particles and the volume of binder in a particle, the agglomerate wetness is able to be estimated using computational geometry.

1 INTRODUCTION

In granulation binder content and binder viscosity interact in complex ways, affecting the consolidation rate and the final extent of consolidation (1). Granule growth is considered to be due to coalescence and breakage, with a system eventually reaching an equilibrium state. Models of growth regard granules as either rigid (2) or plastic (3), but these assume the presence of a continuous layer of liquid at the contact interface. The liquid acts to dissipate some of the collision energy. In plastic collisions, deformation further dissipates the collision energy. Simons and Fairbrother (4) define successful coalescence to have occurred when the rupture energy of a liquid bridge formed between granules is greater than the kinetic energy of impact. None of these models define a realistic liquid surface for granules; instead they rely on assuming a smooth surfaced granule which is covered by a binder of uniform thickness. Thorton and Ning (5) produce a granule with a pseudo realistic appearance, but use an adhesion energy rather than a liquid surface. Thus, there is a need to define a realistic agglomerate surface which is formed from both wet and dry regions. During consolidation, the ratio of these wet to dry regions will change.

In this paper, a description of the algorithm for building agglomerates is detailed, where primary particles are added to the granule one at a time. This is analogous to the layering mechanism where agglomerates increase in size primarily as the result of single primary particle contacts. Due to the stochastic motion of particles in a granulator, primary particles are equally likely to collide with an agglomerate from any direction, and hence the long term average is to produce granules

which are closely packed and spherical. The calculation of the binder fluid surface, along with the respective volume and surface area occupied by the primary particles and binder fluid, is discussed in a later section. In performing these calculations, the probability of agglomerate coalescence is able to be estimated.

In this model, agglomerates consist of primary particles (spheres) and binder fluid, where the fluid is formed by a union of tetrahedral segments. The starting configuration is the tetrahedral arrangement of 4 particles as illustrated in figure 59(a), and additional particles are added to the agglomerate individually. As a new particle is added, fluid segments form between the new particle and existing particles of the agglomerate. The minimum distance between sphere centres is defined by $\sigma = 2R + s$, where R is the radius of the equally sized primary particles and s is the minimum separation between spheres. At a given stage in construction, a matrix S stores the Cartesian coordinates of the primary particles as row vectors, and the fluid surface is defined by three matrices, T, F and E. For each fluid segment, T stores the four vertices of the tetrahedra in terms of indices into S. Each row entry in F defines a fluid surface face, where the first three entries of the row refer to the face vertices as indices into S. Additional information stored in an F entry is the outward pointing normal vector of the face, an estimate point for an additional particle (if the face is subsequently selected to bond to a new particle), and a flag as to whether the face is internal (1) or external (0). Faces become internal when a new particle bonds with the agglomerate, forming new external faces. An edge matrix E is also maintained; this matrix is used for viewing the agglomerate only, and is not involved in the algorithm for adding new particles. The estimate point for a new particle e_i to be added to face f_i is obtained from the geometric mid-point O of the three vertices on the face, and the minimum distance between spheres σ. This yields an estimate point for the added particles $O + n_i H$, where x is the distance from a face vertex to the midpoint, n_i is the normal vector and H is the estimated height above the face, $\sqrt{\sigma^2 - x^2}$.

In the initial case shown in figure 59(a), matrices T, F and E appear as follows ;

$$T_4 = \begin{bmatrix} 1 & 2 & 3 & 4 \end{bmatrix}, \quad F_4 = \begin{bmatrix} 1 & 2 & 3 & n_1 & e_1 & 1 \\ 1 & 3 & 4 & n_2 & e_2 & 1 \\ 1 & 2 & 4 & n_3 & e_3 & 1 \\ 2 & 3 & 4 & n_4 & e_4 & 1 \end{bmatrix}, \quad E_4 = \begin{bmatrix} 1 & 2 \\ 1 & 3 \\ 1 & 4 \\ 2 & 3 \\ 2 & 4 \\ 3 & 4 \end{bmatrix},$$

where n_i is the outward pointing normal vector of face i, e_i is the estimate point for a new particle on face i, and the final column of F indicates that all faces are external for the initial arrangement. The subscript N on the T, F and E matrices refer to the matrices for an N particle agglomerate.

When adding a fifth particle to face with index 1 (face [1 2 3]), a new tetrahedron is added, face 1 becomes internal, and 3 faces and 3 edges are added. Figure 59 shows the original (or base) tetrahedron for the 4 particle case on the left, and the 5 particle case is shown on the right. Following the addition of the 5th particle, matrices T, F, and E are updated as follows ;

$$T_5 = \begin{bmatrix} 1 & 2 & 3 & 4 \\ 2 & 3 & 4 & 5 \end{bmatrix}, \quad F_5 = \begin{bmatrix} 1 & 2 & 3 & n_1 & e_1 & 0 \\ 1 & 3 & 4 & n_2 & e_2 & 1 \\ 1 & 2 & 4 & n_3 & e_3 & 1 \\ 2 & 3 & 4 & n_4 & e_4 & 1 \\ 5 & 1 & 2 & n_5 & e_5 & 1 \\ 5 & 1 & 3 & n_6 & e_6 & 1 \\ 5 & 2 & 3 & n_7 & e_7 & 1 \end{bmatrix}, \quad E_5 = \begin{bmatrix} 1 & 2 \\ 1 & 3 \\ 1 & 4 \\ 3 & 4 \\ 2 & 3 \\ 2 & 4 \\ 1 & 5 \\ 2 & 5 \\ 3 & 5 \end{bmatrix}.$$

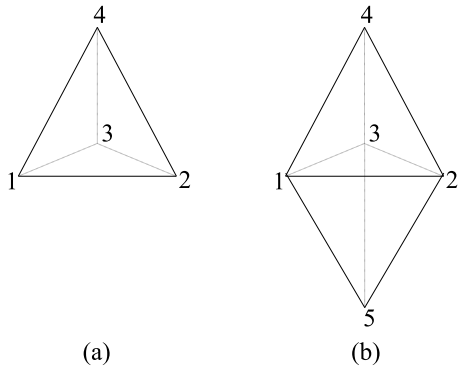

Figure 59: The tetrahedron on the left defines placement of the spheres for primary particles 1-4. When a 5th particle is added, the arrangement is given by the 2 tetrahedra (as on the right).

2 AGGLOMERATE GROWTH ALGORITHM

Agglomerates grow by adding particles to an existing agglomerate. To maintain spherical growth behaviour, the incoming particle approaches the first external face $f \in F$, as this is approximately the closest external face to the centre of the agglomerate. In the simple case where the addition of a particle results in the formation of one new tetrahedra, the coordinates of the new particle are given by the estimate position for face f, e_i. In more complex cases, the incoming particle forms contact with more than one face, resulting in more than one tetrahedra. The new particle position is then given by the solution to an optimisation problem which is discussed later. Tests with all neighbouring faces of f are used to determine how many tetrahedra are to be added as a result of the new particle. The test consists of two scenarios which are compared on the basis of the regularity of the resulting tetrahedra. The first scenario, illustrated in figure 60(a), places the new particle between face f and the neighbour creating two tetrahedra. The average skewness of the tetrahedra is calculated using the method discussed below. The second scenario shown in figure 60(b) positions two particles between the faces, resulting in three tetrahedra and the average skewness is again calculated. If the average skewness of scenario two is lower than that of one for all neighbouring faces to f, i.e. if it is more optimal to place two particles between f and its neighbours, then only one new tetrahedra is formed and the particle is placed in position e_i. An example of this case is shown in figure 61. If the skewness in scenario one is lower for any pair in the test, then the neighbour to f is added as a face which will bond with the new particle. This neighbouring face then tests its own neighbours pairwise (excluding the parent) using the skewness criteria, which may result in additional faces that bond with the new particle. The set of faces that bond with the new particle are known as contact faces, and form the bases of the new tetrahedra which are to be added. Spheres which share their vertices with the contact faces, and which bond with the new particle, are known as contact spheres.

A quantity called the skewness number κ is introduced to test the regularity of added tetrahedra. This number measures how much a proposed tetrahedron with volume V_{tetra} deviates from a regular (or ideal) tetrahedron of the same volume. A regular tetrahedron has $\kappa = 0$, with larger skewness numbers implying that the given tetrahedron deviates more strongly from the ideal shape. The volume of the given tetrahedron is calculated using

$$V_{\text{tetra}} = \frac{1}{6}|a \cdot b \times c| \tag{2.75}$$

where a, b, c are vectors from one vertex of the new tetrahedron to the other vertices. Using the equation for the volume of a regular tetrahedron, the ideal edge length (of a regular tetrahedron)

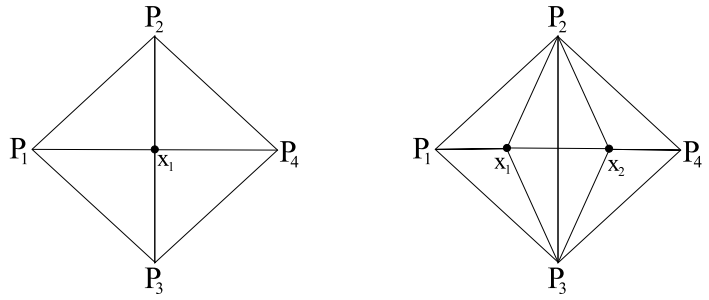

(a) Determining the point to place particle x_1 in the one particle case.

(b) Determining the point to place particles x_1 and x_2 in the two particle case.

Figure 60: Adding a single particle (a), or two particles (b) between neighbouring faces l (with vertices P_1, P_2, P_3) and m (with vertices P_2, P_3, P_4).

can be calculated as

$$L_{\text{ideal}} = \left(\frac{12}{\sqrt{2}} V_{\text{tetra}} \right)^{\frac{1}{3}}. \tag{2.76}$$

The non-dimensional skewness number κ measures the deviation in length of the 6 edges from L_{ideal},

$$\kappa = \frac{\sum_{i=1}^{6} |L_i - L_{\text{ideal}}|}{L_{\text{ideal}}}. \tag{2.77}$$

Figure 60(a) shows the case where one particle is added at position x_1 to face f with vertices P_1, P_2 and P_3, and a neighbour with vertices P_2, P_3 and P_4. As two tetrahedra are added for this case, the volume of both tetrahedra V_{tetra1} and V_{tetra2} are calculated using equation (2.75). The vectors a, b and c for f may be given as $a = P_2 - P_1$, $b = P_3 - P_1$ and $c = x_1 - P_1$, and as $a = P_2 - P_4$, $b = P_3 - P_4$ and $c = x_1 - P_4$ for the neighbour. Corresponding to V_1 and V_2, the skewness numbers κ_1 and κ_2 are evaluated using equation (2.77), and their average is taken as κ. For the two particle case in figure 60(b), three tetrahedra are required. The case with the lower skewness number determines whether one or two particles are to be added between the faces.

In order to determine the coordinates of the spheres x_1 and x_2 (shown in figure 60), an optimisation problem is solved using MATLAB 6.5. For the one particle case of bonding, the total bond length between the new particle and P_1, P_2, P_3 and P_4 is to be minimised, such that the length of the bonds is at least σ. The objective function to be minimised is

$$\Psi = \sum_{i=1}^{4} |x_1 - P_i|,$$

with constraints on the bond length as $|x_1 - P_j| \geq \sigma$ for $j = 1, 2, 3, 4$.

For the two particle case, geometrically we have the face as shown in 60(b) with four vertices, P_1, P_2, P_3, P_4. The optimal placement of the two particles, shown as x_1 and x_2 in the figure, are unknown coordinates to be determined by optimisation. To minimise the total bond length, the objective function is

$$\Psi = \sum_{i=1}^{3} |x_1 - P_i| + \sum_{j=2}^{4} |x_2 - P_j| + |x_1 - x_2|.$$

As constraints, it is required that the length of the bonds must be at least σ, the separation distance between sphere centres, i.e. $|x_1 - P_j| \geq \sigma$ and $|x_2 - P_j| \geq \sigma$ (for $j = 1, 2, 3, 4$) and $|x_1 - x_2| \geq \sigma$. A

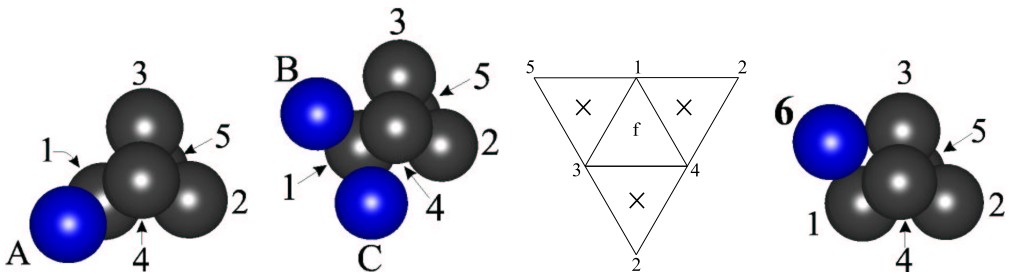

(a) Sphere A is the position for placing one particle between faces [1 3 4] and [1 2 4].

(b) Spheres B and C are the placement for two particles between faces [1 3 4] and [1 2 4].

(c) Diagram of the contact faces.

(d) The actual position for the 6th sphere, as determined by optimisation.

Figure 61: Adding a particle to a 5 particle agglomerate. A contact face comparison between faces [1 3 4] and [1 2 4] is shown in figures (a) and (b). A single contact face exists for this case ([1 3 4]), with contact spheres 1, 3 and 4. Figure (c) illustrates the placement of the new particle.

non-linear equality constraint is specified in which $|x_i - P_1| = |x_j - P_4| = |x_1 - x_2|$. The starting values of x_1 and x_2 are given by using the estimate points e_l and e_m (corresponding to faces l and m) in matrix F.

Once the optimisation above is complete, the tetrahedra to be added are known; the new tetrahedra are appended to matrix T, the new faces are added to F (and the flag changed from external to internal for existing faces on F), and the position of the new sphere is appended onto matrix S.

3 EXAMPLE OF PARTICLE PLACEMENT

Figure 61 illustrates the algorithm discussed in the previous section when adding a primary particle to a 5 particle agglomerate. The original primary particles are labelled '1'-'5' in figures 61(a)-(c) and the initial contact face is f = [1 3 4]. Figures 61(a) and 61(b) consider a contact face comparison between this face and neighbouring face [1 2 4]. The sphere labelled 'A' in figure 61(a) is the position as determined by optimisation when adding one particle between the faces. In figure 61(b) spheres 'B' and 'C' are the optimal placement when adding two spheres between the faces. For the one particle case in 61(a), the tetrahedra required are [1 3 4 A] and [1 2 4 A]. By calculation, these tetrahedra have an average skewness of $\kappa_1 = 1.83$ (to 2 d.p.). For the two particle case in 61(b), three tetrahedra are required, [1 3 4 B], [1 4 B C], and [1 4 C 2], which have an average skewness of $\kappa_2 = 0.36$. Since $\kappa_2 < \kappa_1$, it is more optimal for two particles to be added between the faces, hence face f = [1 2 4] is not included as a contact face. Similarly, the other neighbours to [1 3 4], faces [2 3 4] and [5 1 3], also yield $\kappa_2 < \kappa_1$. Hence there is one contact face with contact spheres 1, 3 and 4. Figure 61(d) shows the actual placement for the sixth particle.

4 CALCULATION OF THE FLUID SURFACE

The distribution of liquid within an agglomerate is able to be represented using two parameters of the model, the separation distance between spheres σ and a saturation parameter δ. The fluid surface is formed using these parameters, along with the tetrahedra T and S matrices where for each row $t \in T$ a fluid segment is formed. The non-dimensional saturation parameter δ ($0 \leq \delta \leq 1$) is used to adjust the position of the external faces of the tetrahedron, allowing a variable amount of

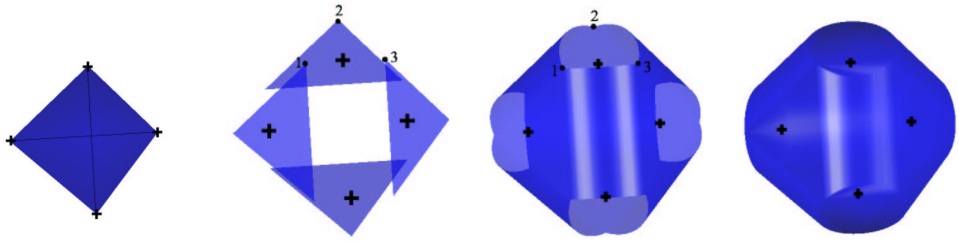

(a) The unexpanded binder tetrahedra, corresponding to $\delta = 0$

(b) Fluid tetrahedra, expanded by $\delta = 0.7$.

(c) Cylinders added to saturation state $\delta = 0.7$.

(d) Half-space cuts are used to produce an object which is closed off.

Figure 62: Creation of a binder fluid segment

volume to exist within the agglomerate. The state $\delta = 0$ corresponds to a non-expanded state, in which the fluid surface is connected to the centres of the primary particles. For higher saturation states, $\delta > 0$, the fluid surface is defined by moving the external faces of the tetrahedron in the direction of their outward pointing normal vectors, up to a maximum saturation state of $\delta = 1$. A saturation of $\delta = 1$ corresponds to the case where the faces are moved outward a distance R equal to the radius of the spheres. Figure 62(a) shows the unexpanded state $\delta = 0$, while figure 62(b) illustrates the saturation state $\delta = 0.7$. The location of the primary particles remain fixed as the saturation state is varied; the points '+' shown in figure 62 correspond to the centre points of the primary particles. In all but the $\delta = 0$ case, cylinders of radius δ connect adjacent faces together along the edges of the tetrahedron as shown in figure 62(c). k points along each of the cylinders link adjacent faces of the tetrahedron together. Triangular mapping is used to form the vertices and faces of the cylinders. The value of k is called the polyhedra accuracy. Once the cylinders are added, the first derivative of the surface is continuous, but discontinuities in the second derivative occur where cylinders intersect with the faces of the tetrahedron. As a result the fluid segments do not have constant mean curvature, and therefore the fluid surface is an approximation to the true binder surface.

As discussed in section 5, the binder fluid segments T_i must be convex objects. This is achieved by forming the object as above, and then closing off the object by intersecting with planes that pass through the lowest points of the expanded faces (the points 1, 2 and 3 in figures 62(b) and 62(c)). The completed binder segment is shown in figure 62(d).

5 AGGLOMERATE PROPERTIES

In this section, some concepts are introduced which enable agglomerate properties, which include the surface area, volume, and fraction of wetted surface area, to be evaluated. An agglomerate is the non-convex union of n_S primary particles with n_T tetrahedra, or

$$(\bigcup_{i=1}^{n_S} S_i) \cup (\bigcup_{i=1}^{n_T} T_i). \tag{5.78}$$

Although these properties can only be evaluated for convex objects, the non-convex union in equation (5.78) can be written in terms of convex sets. This is achieved by taking unions and differences of the convex sets S_i and T_i (as unions and differences of convex sets are also convex). Convex sets are able to be written as a collection of half-spaces; a half-space is defined as

$$n \cdot (x - x_0) \leq 0 \quad (n \neq 0), \tag{5.79}$$

where $n \in \mathbb{R}^3$ is an outward pointing normal vector and $x_0 \in \mathbb{R}^3$ is a point that lies on the plane

$$n \cdot (x - x_0) = 0 \quad (n \neq 0). \tag{5.80}$$

It is common to define $d = n \cdot x_0$. Using d, equation (5.79) is written

$$n \cdot x \leq d \quad (n \neq 0). \tag{5.81}$$

A polyhedron is a bounded convex set formed by the intersection of a finite number of half-spaces; the spheres S_i are polyhedra, and the construction of the T_i objects (discussed in section 4) is such that the fluid segments are polyhedra. As a half-space is convex, and since intersections between convex regions are convex, polyhedra are convex. Properties of polyhedra including the surface area and volume can be calculated. In general, the volume of non-convex objects can only be evaluated by first dividing the object into convex regions, and summing properties of the convex portions piecewise. For a union of convex components A_i,

$$\bigcup_i A_i = \sum_i A_i - \sum_{i \neq j} A_i \cap A_j + \sum_{i \neq j \neq k} A_i \cap A_j \cap A_k - \ldots \pm \bigcap_i A_i. \tag{5.82}$$

Since polyhedra are an intersection of half-spaces, the intersection of two or more overlapping polyhedra is also a polyhedra. The union in equation (5.82) requires polyhedra intersections to be evaluated.

Construction of the agglomerate (sphere placement, binder fluid placement, and matrices S, T and F) are completed using MATLAB . Computational geometry calculations were completed using an external C++ mathematics library written by Jonathan Marshall[3]. The library includes routines to calculate the intersection between two polyhedra (e.g. P_1 and P_2 producing $P_1 \cap P_2$), the intersection of a polyhedra P with a half-space, and the calculation of area and volume of polyhedra.

6 CALCULATING SURFACE AREA, VOLUME AND THE WETNESS

The wetness W is defined as the wetted fraction of the exterior agglomerate surface area. As W is the fraction of binder fluid accessible to other incident particles, it is proposed that when two agglomerates collide the probability of coalescence is related to the wetness of both agglomerates. Exactly how the agglomerate wetness relates to coalescence is not examined in this paper.

The wetness of agglomerates is calculated using variables A_{wet} and A_{dry} which refer to wet and dry surface areas of the particle. Primary particles drawn on the binder surface of figure 62(d) are shown in figure 63(a). In this figure, the total agglomerate surface area $A = A_{\text{dry}} + A_{\text{wet}}$ is the sum of the exposed surface area of the spheres and the binder fluid. For the 4 particle case, the polyhedra that result from the intersection of the primary particles and binder fluid are shown in figure 63(b). A_{wet} is calculated as the area of the binder less the area of the intersected polyhedra common to the binder, and A_{dry} is equal to the area of the spheres less the area of the intersected polyhedra common to the spheres. The wetness W is equal to

$$W = \frac{A_{\text{wet}}}{A_{\text{wet}} + A_{\text{dry}}}. \tag{6.83}$$

The primary particles of a 4 particle agglomerate are drawn in figure 63(a), along with the fluid tetrahedron T_1. Dry regions are the sphere portions (where they do not overlap with the fluid), and the binder tetrahedron is wet (where it does not overlap with the spheres). Later, the wetness is plotted as a function of the volume ratio of binder fluid to solids. The solids volume is simply

[3]Institute of Fundamental Sciences, Massey University, New Zealand

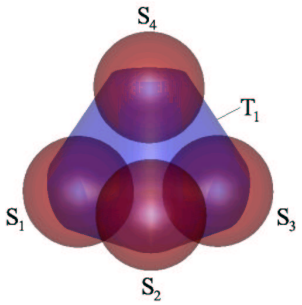

(a) A 4 particle agglomerate, showing placement of primary particles and binder fluid.

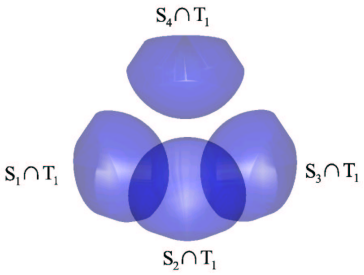

(b) Polyhedra resulting from the intersection between primary particles and binder fluid.

Figure 63: In figure 63(a), primary particles and the binder tetrahedra is drawn. Figure 63(b) shows the intersected portions, obtained by intersecting the spheres with the binder fluid. For this figure, $R = 1$, $\delta = 0.7$ and $s = 0.5$.

$N \times \frac{4}{3}\pi R^3$, and the binder volume V_{wet} is calculated using the volume of the tetrahedra and the volume of the intersected regions such that (for the 4 particle case in figure 63)

$$V_{\text{wet}} = V(T_1) - \sum_{i=1}^{4} V(S_i \cap T_1)$$

where $V(P)$ is the volume of polyhedron P. The fluids to solids ratio between V_{wet} and the volume of solid is denoted V^*. For the surface areas, A_{dry} and A_{wet} are

$$A_{\text{wet}} = A(T_1) - \sum_{i=1}^{4} A_{\text{wet}}(S_i \cap T_1) \text{ and } A_{\text{dry}} = \sum_{i=1}^{4} [A(S_i) - A_{\text{dry}}(S_i \cap T_1)] \tag{6.84}$$

where $A_{\text{dry}}(S_i \cap T_1)$ is the area of $S_i \cap T_1$ (see figure 63(b)) common to S_i, and $A_{\text{wet}}(S_i \cap T_1)$ is the area of $S_i \cap T_1$ (see figure 63(b)) common to T_1. The wetness is calculated using equation (6.83).

7 CUTTING THE TETRAHEDRA

For saturation states $\delta > 0$ neighbouring tetrahedra overlap when formed using the method of section 4. For large agglomerates, large number of overlaps occur between the tetrahedra and the primary particles. Figure 64(a), for example, shows the 5 particle case where overlap occurs between 2 fluid tetrahedra. The number of intersections required to calculate the union of equation (5.78) (as implied by equation (5.82)) are able to be minimised if overlap is not permitted between the fluid segments, i.e. if $T_i \cap T_j = \emptyset$ for $i \neq j$. If this is enforced, then since $S_i \cap S_j = \emptyset$ for $i \neq j$, then the only non-empty intersections are $S_i \cap T_j$. This reduces the agglomerate union of equation (5.78) to

$$\sum_i S_i + \sum_i T_i - \sum_{i \neq j} S_i \cap T_j. \tag{7.85}$$

Therefore, when adding a tetrahedron T_k, existing tetrahedra which neighbour T_k along with T_k are cut to avoid overlap. Depending on how many vertices are shared between indices of T_k and the neighbour, different half-space cuts are completed. If a face is shared with 3 common (primary

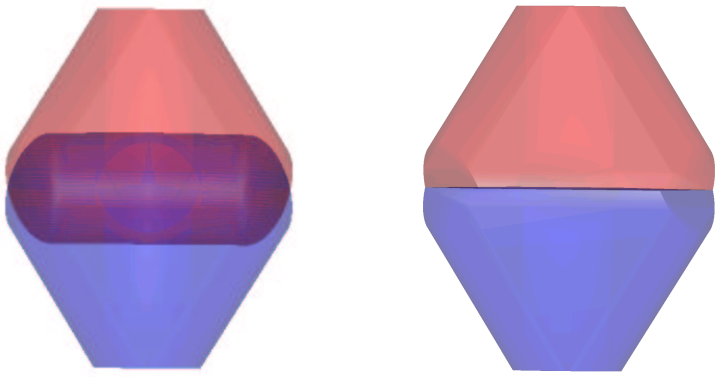

(a) The tetrahedra fluid segments overlap for $N = 5$ primary particles.

(b) Cutting the tetrahedra with the appropriate half-spaces resolves this, and enables the wetness to be calculated.

Figure 64: Overlap at a face for two adjacent tetrahedra. Primary particles are not drawn in this figure.

particle) vertices, a face cut is completed, an edge cut is made if an edge is shared and 2 vertices are common, and a point cut is made if there is one vertex in common.

In the situation shown in figure 64(a), the tetrahedra meet at a face and 3 vertices are shared. Denote the red (or top) tetrahedron as T_1, the blue tetrahedron as T_2, and the face shared by the tetrahedra as f. As primary particles common to T_1 and T_2 lie in the plane of f, f is the appropriate dividing plane to cut the tetrahedra. Cuts are also performed when the binder tetrahedra overlap due to edge and point cuts.

8 RESULTS OF THE MODEL

Parameters for the model are the number of primary particles N, the minimum sphere separation distance between spheres s and the fluid saturation parameter δ. Using these parameters, the surface wetness, area and volume are calculated as follows:

$$W = W(N, s, \delta) \text{ and } V^* = V^*(N, s, \delta), \tag{8.86}$$

where N is the number of primary particles and V^* is the fluid to solid ratio. Assumptions for the model are that the primary particles are non-deformable rigid spheres and that the binder is distributed uniformly beneath the fluid surface, that is, the agglomerate is in the capillary state. In the results presented a normalised sphere radius of $R = 1$ is used, with the polyhedra accuracy k (as discussed in section 4) set equal to 30. The parameters s and δ are calculated over the ranges of $s = 0 : 0.01 : 1$ and $\delta = 0 : 0.01 : 1$[4]. For an N particle agglomerate, surfaces parameterised by s and δ are obtained for each of the functions from equation (8.86).

In granulation systems when a measured amount of powder and binder are mixed, the fluid to solid ratio V^* is a known quantity. If it is assumed that no evaporation occurs, and that the solid particles are rigid spheres, then V^* is constant for a given system. Consolidation occurs over time and so the separation distance between primary particles decreases. Of interest is the relationship between surface wetness W and the separation distance s for constant V^*. In the following section, the relationship between these variables is studied.

[4] $a : b : c$ is the set $\{a, a + b, a + 2b, ..., c\}$, where $\frac{c-a}{b}$ steps exist between a and c.

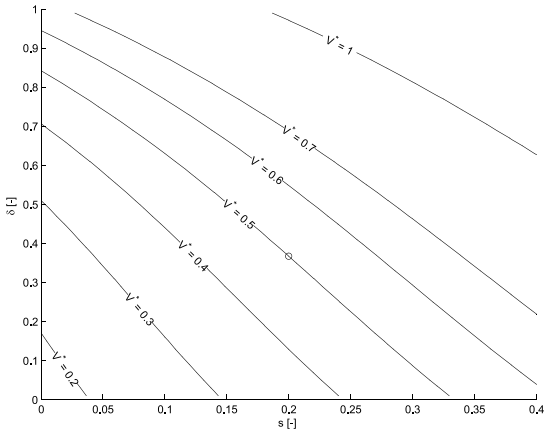

Figure 65: Volume contour plot showing the variation of the parameters s and δ for constant fluid to solid ratio V^* for a 30 particle agglomerate. The fluid to solid ratio is considered for $V^* = 0.2 : 0.1 : 0.7$ and $V^* = 1.0$

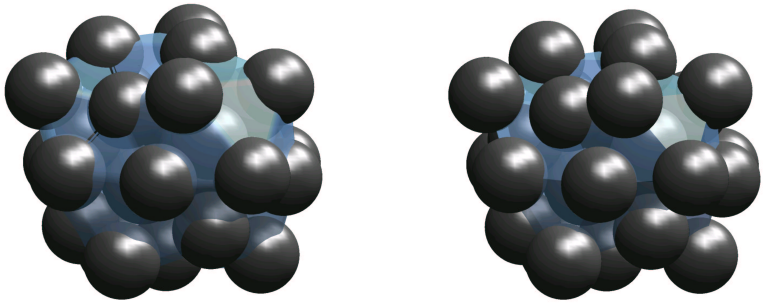

(a) The agglomerate formed for $N = 30$, $s = 0.2$ and $\delta \approx 0.37$.

(b) The agglomerate formed for $N = 30$, $s = 0.2$ and $\delta = 0$.

Figure 66: Two saturation states of an agglomerate formed by 30 primary particles with minimum separation distance between spheres $s = 0.2$. Plot (a) corresponds to the case represented as a circle ('o') in figure 65, with $\delta \approx 0.37$, $V^* \approx 0.5$ and $W \approx 0.27$. Plot (b) shows the state $\delta = 0$, with $V^* \approx 0.36$ and $W \approx 0.16$.

9 SURFACE WETNESS ANALYSIS

The mechanism by which consolidation occurs has been studied by workers including (3), but is not considered in this study. Given that agglomerates consolidate, this work investigates the change in surface wetness W that results from a decrease in the inter-particle separation distance s. The relationship between s and δ for fixed values of the fluid to solid ratio V^* for a 30 particle agglomerate is shown in figure 65 for $V^* = 0.2 : 0.1 : 0.7$ and $V^* = 1.0$. A particular agglomerate is defined by fixing three of the parameters of the model; the complete set of parameters is W, A^*, V^*, N, δ and s. An example is given in figure 66(a), where the fixed parameters are $N = 30$, $s = 0.2$ and $V^* = 0.5$. In the contour plot of figure 65, this configuration is shown as a circle ('o') on the $V^* = 0.5$ contour. Using the functions V^* and W, the liquid saturation state for this example is $\delta \approx 0.37$ and the surface wetness is $W \approx 0.27$, implying that approximately 27% of the agglomerate is surface wet. For a fixed inter-particle separation distance, the surface wetness increases with increasing fluid to solid ratio V^*, which agrees with intuition.

Figure 67 shows a plot of surface wetness W with respect to separation distance s for a range of V^* values. Dashed contours on this figure represent constant values of the liquid saturation parameter δ. The figure shows that for decreasing separation distance s, an increase in the surface wetness W occurs for constant V^*. This can be understood by considering an N particle agglomerate in a expanded (or loosely-packed) state, with separation distance s_1. When consolidation occurs, and the separation distance is decreased from s_1 to s_2, the void volume of the agglomerate reduces. This forces the fluid to migrate from the interior of the particle to the agglomerate surface, which has the effect of increasing the surface wetness.

Figure 69 shows the trend of surface wetness with respect to inter-particle separation distance for different sized agglomerates; in particular for $N = 10, 20, 30$ and 50. Several different values of the fluid to solid ratio V^* are shown in each of the plots of 69(a)-69(d). For fixed N, the surface wetness increases for decreasing separation distance s, as discussed above. For fixed inter-particle separation distance s, and for a particular V^*, the figure shows decreasing surface wetness for increasing numbers of primary particles (N). This behaviour can be explained by introducing the commonly used voidage ϵ, which is defined, for the maximal saturation state $\delta = 1$, as

$$\epsilon = \frac{V_{\text{wet}}}{V_{\text{wet}} + N \times \frac{4}{3}\pi R^3}, \tag{9.87}$$

where V_{liquid} is the volume of binder fluid in an agglomerate normalised to the volume of a primary particle, and V_{solid} is equal to N (as V_{liquid} and V_{solid} are normalised to the volume of a sphere of radius R). The voidage calculation given in equation (9.87) is akin to 'wrapping' the surface of the particle with cellophane, and then calculating the fraction of volume occupied by liquid. Figure 68 shows the relationship between voidage and the inter-particle separation distance s, which shows that, for fixed s, voidage ϵ increases with increasing N. As more particles are added to the agglomerate (increasing the radius of the particle), more void space is introduced. The result shown in figure 68 suggests that the void (internal) volume increases as the particle increases in radius. As there is proportionally more volume interior to the agglomerate, more binder fluid exists inside the particle and this reduces the surface wetness of the agglomerate. Figure 70 considers the relationship plotted in figure 67 for varied number of primary particles N. In general, for constant V^*, this figure shows that small agglomerates are the most surface wet with surface wetness decreasing as more primary particles are added.

The contours of wetness in figures 67 and 69 have an upper limit with respect to W due the idealised model described in section 4, where saturation has a maximum value of $\delta = 1$. In reality, for such super-saturated states (i.e. for $\delta > 1$) the fluid would completely enclose the primary particles to form a slurry, but this is of no interest in granulation. Conversely, for dry particles, the wetness may be less than those given in figure 67 which correspond to $\delta = 0$. The value $\delta = 0$ is not a physical limit, but is a model limit due to the methods described in section 4 to construct the binder surface.

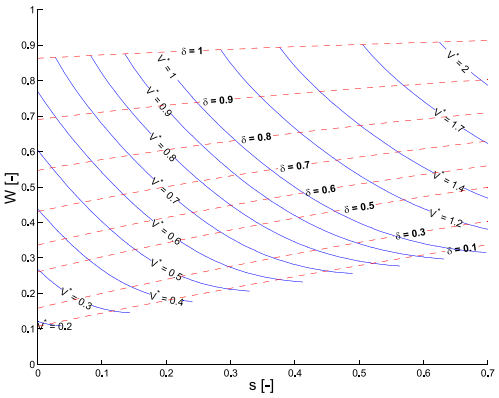

Figure 67: Volume contour plot of surface wetness W with respect to separation distance s for an $N = 30$ particle agglomerate. Solid lines denote constant values of V^*, while dashed lines are contours of constant δ.

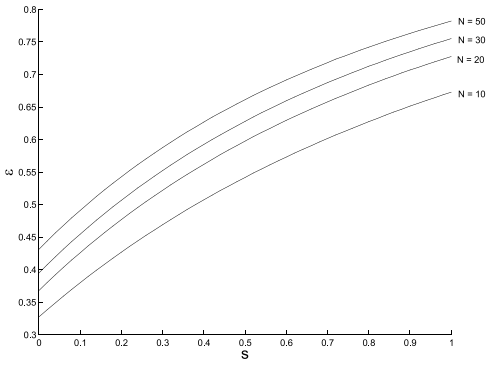

Figure 68: Plot of voidage ϵ with respect to s. For fixed s, the voidage increases for increasing particle number N.

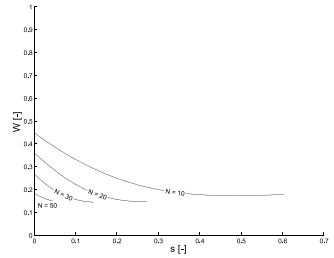

(a) $V^* = 0.3$

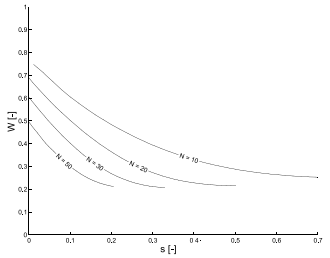

(b) $V^* = 0.5$

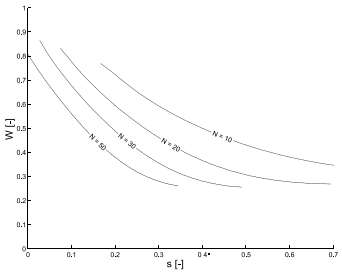

(c) $V^* = 0.7$

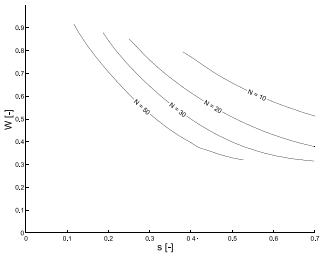

(d) $V^* = 1.0$

Figure 69: Plot of surface wetness W with respect to inter-particle separation distance s for agglomerates composed of 10, 20, 30 and 50 primary particles. Values of V^* used in this figure are $V = 0.3, 0.5, 0.7$ and 1.0.

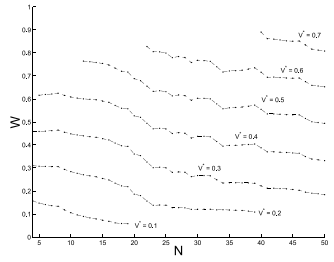

(a) $s = 0$

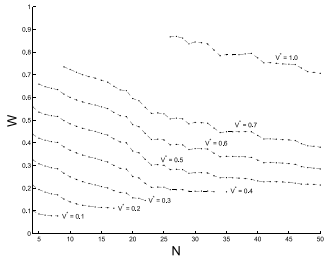

(b) $s = 0.2$

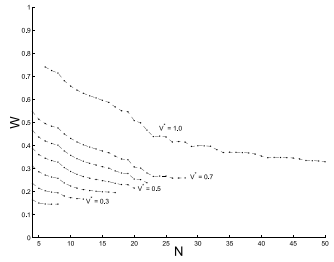

(c) $s = 0.5$

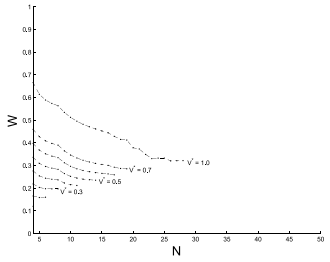

(d) $s = 0.7$

Figure 70: Graphs of wetness W with respect to particle number N for a range of s and a range of fluids to solid ratio values V^*.

10 CONCLUSIONS

The following conclusions can be drawn from this model about surface wetness as a function of the number of primary particles in the agglomerate, the separation distance of these particles, and the saturation of the agglomerate.

- small agglomerates are the most surface wet for a constant separation distance, and large agglomerates have a lower surface wetness.
- as the separation distance decreases during consolidation, and for constant values of the fluids to solids volume ratio V^* the, wetness increases.
- the rate of change of wetness increases with further consolidation.
- agglomerates with larger fluids to solids volume ratio have greater surface wetness.

11 ACKNOWLEDGEMENT

The authors wish to thank Jonathan Marshall, Institute of Fundamental Sciences, Massey University, for developing the computational geometry toolbox used in this project. A short description of the routines used was discussed in section 5.

References

[1] Simon M. Iveson, James D. Litster, Karen Hapgood and Bryan J. Ennis. Nucleation, growth and breakage phenomena in agitated wet granulation processes: a review. *Powder Technology*, 117:3–39, 2001.

[2] B.J. Ennis, G.I. Tardos, R. Pfeffer. A microlevel based characterisation of granulation phenomena. *Powder Technology*, 65:257–272, 1991.

[3] L.X. Liu, J.D. Litster, S.M. Iveson, B.J. Ennis. Coalescence of deformable granules in wet granulation processes. *American Institute of Chemical Engineers*, 46:529–539, 2000.

[4] S.J.R. Simons and R.J. Fairbrother. Direct observations of liquid binder-particle interactions: the role of wetting behaviour in agglomerate growth. *Powder Technology*, 110:44–58, 2000.

[5] C. Thornton and Z. Ning. A theorectical model for the stick/bounce behaviour of adhesive, elastic-plastic spheres. *Powder Technology*, 99:154–162, 1998.